

MDPI

Article

Study on Fire Smoke Movement Characteristics and Their Impact on Personal Evacuation in Curved Highway Tunnels

Yuang Cui D and Zhiqiang Liu *

School of Civil Engineering, Lanzhou Jiaotong University, Lanzhou 730070, China; 11220166@stu.lzjtu.edu.cn * Correspondence: lzqiang@mail.lzjtu.cn

Featured Application: Featured Application: Fire Dynamics Simulator Pyrosim.

Abstract: In the existing research on tunnel fires, researchers primarily focus on straight tunnels, neglecting the impact of curved sidewalls in curved tunnels. Based on the theory of smoke diffusion, a series of CFD numerical simulations was conducted using the Fire Dynamics Simulator to investigate the characteristics of smoke distribution in a curved highway tunnel. The results indicated that distinct smoke distribution characteristics were observed when a fire occurred in a curved tunnel compared with those observed in straight tunnels, with significant differences particularly evident for the radius of curvature of the tunnel below 1000 m. By comparing the smoke distribution characteristics from various fire source locations, the most unfavorable fire source locations within a curved tunnel were determined. High-temperature fire smoke bounds between the inner and outer walls of the tunnel, leading to the formation of multiple high-temperature zones in proximity to the fire source, rather than diffusing directly towards the exit in a linear tunnel. Additionally, based on an analysis of temperature, visibility, and CO concentration at characteristic heights, suitable locations for pedestrian crossings within the tunnel were deduced and an evacuation strategy for persons within the core fire area was proposed. The results can provide a reference for personal evacuation strategies in curved highway tunnel fire scenarios and the design of an adit for people passing in such tunnels.

Keywords: curved highway tunnel; fire; smoke distribution; personal evacuation



Citation: Cui, Y.; Liu, Z. Study on Fire Smoke Movement Characteristics and Their Impact on Personal Evacuation in Curved Highway Tunnels. *Appl. Sci.* 2024, 14, 6339. https://doi.org/10.3390/app14146339

Academic Editor: Cheng-Yu Ku

Received: 22 June 2024 Revised: 15 July 2024 Accepted: 18 July 2024 Published: 20 July 2024



Copyright: © 2024 by the authors. Licensee MDPI, Basel, Switzerland. This article is an open access article distributed under the terms and conditions of the Creative Commons Attribution (CC BY) license (https://creativecommons.org/licenses/by/4.0/).

1. Introduction

With the advancement of tunnel excavation technology, there has been a gradual increase in the proportion of curved highway tunnels within highway systems. The unique structure of a curved tunnel introduces greater complexity to smoke flow and temperature variations during fire incidents, depending on the radius of the tunnel turn [1–3]. Previous research has delineated the movement patterns of fire smoke in linear tunnels and provided formulas to calculate the length of smoke back-layer, critical wind speed, and maximum temperature. However, the diffusion of smoke is subject to various influencing factors such as altitude, slope gradient of the tunnel, and tunnel curvature. Tunnel curvature constitutes the focus of this investigation.

Previous research has demonstrated that curved tunnels and straight tunnels exhibit distinct characteristics. Kashef et al. studied the smoke control strategy in the straight-line and curved areas of a tunnel through experiments and numerical simulations. Their results pointed out that when the fire source was in the curved area, the temperature near the fire source was significantly lower than that in the straight area and the smoke back-layer length increased [4].

Meanwhile, correction formulas have been proposed for key indicators of curved tunnel fires based on those of straight tunnel fires. Wang Feng constructed numerical models on the fire smoke movement characteristics of a curved tunnel with a radius of

600 m and proposed a calculation method of the resistance along the curve tunnel to clarify the law of the influence of the curved tunnel on the fluid flow [5–7]. Caliendo et al. used CFD numerical simulation to study the influence of longitudinal ventilation on smoke backlayering in a two-lane curved tunnel and predicted the location of the maximum ceiling temperature [8]. Wu et al. studied the fire smoke transport characteristics of the Qianhaizi curve highway tunnel to obtain the critical wind speed of the tunnel [9]. Wang conducted numerical simulations of a curved road tunnel fire using Fluent to compare the critical wind velocity at the convex and concave locations of the fire source. They also analyzed the length of the smoke back-layering and concluded that the critical velocity at the convex location was larger [10]. Zhong et al. studied the law of smoke spread during fires in inclined and curved tunnels by numerical simulations and experiments and found that the location with the greatest difference in heat transfer rates was the tunnel ceiling under different working conditions [11]. Zhang et al. combined numerical simulation with theoretical analysis to determine a fire model suitable for curved tunnels and studied the length of the smoke layer and critical ventilation velocity of curved tunnels [12]. Pan et al. studied the effect of a curved sidewall on the fire shape and maximum temperature beneath the ceiling centerline and established formulas to predict the maximum temperature beneath the ceiling centerline [13]. Lu investigated the temperature distribution in curved tunnels through a numerical simulation method and proposed a new exponential decay model for longitudinal temperature predictions under various tunnel curvature conditions [14]. Xu et al. conducted experiments and numerical simulations to analyze the critical velocity of a curved tunnel under different fire scenarios [15].

Nevertheless, there remains little research directly investigating the impact of fire in curved tunnels on personal evacuation. Muhasilovic et al. studied the influence of the curvature radius (>2500 m) on thermal radiation and smoke distribution in a tunnel through numerical simulation [16]. Lu established a numerical model by FDS to compare the smoke diffusion and temperature distribution of a tunnel fire in the straight section and the curved section. They found that the smoke backflow was more serious and the temperature increased more significantly when the fire occurred in the curved section [17]. Zhao et al. used FDS to conduct a numerical simulation of a tunnel fire with a small curvature radius and found that the curvature radius would lead to a large temperature gradient near the fire source [18]. Li simulated the fire smoke flow in a single curvature tunnel by Fluent to obtain the change in CO concentration under different curvature and ventilation environments [19]. Liu et al. evaluated factors such as tunnel curvature, longitudinal ventilation operation time, and ventilation velocity in order to investigate the influence of longitudinal ventilation parameters on the fire-extinguishing effect of water mist in a curved tunnel [20].

Moreover, the characteristics of smoke diffusion at the characteristic height of the human eye and the variation in factors such as temperature, visibility, and CO concentration in curved tunnel fires that affect personal evacuation have not been realized. Even the existing codes lack specific guidelines for fire control in curved tunnels [21,22]. This paper thus ascertains the characteristics of smoke diffusion exhibited by curved highway tunnels with varying curvatures and assesses the impact on personal evacuation. The recommended evacuation strategies and design of an adit for people are also provided. The focus lies on the distinct smoke diffusion pattern and strategies to deal with its impact on evacuations.

2. Materials and Methods

2.1. Fire Dynamics Simulator

The Fire Dynamics Simulator (FDS) [23,24] is code developed by the U.S. National Institute of Standards and Technology that has been widely adopted by many researchers to study temperature and velocity fields in fires following the maturation of computational fluid dynamics (CFD) and the development of computer computing ability [25]. The validity of this code has been extensively verified by many works in fire research. The FDS is designed for large-eddy simulation (LES) of low-velocity and thermal-driven flows, and

the new version (Version 6) offers many advances in hydrodynamics, turbulence models, and scalar transport schemes. Thus, the FDS (Version 6.8) with an LES model is adopted in this study. More details about the FDS can be referred to McGrattan et al. [26]. The feasibility of FDS used to simulate the tunnel fire behaviors has been verified by previous studies [27,28].

2.2. Fire Scenario Analysis

As shown in Figure 1, a full-scale tunnel model with a center line length of 1000 m is established in this study. The tunnel section is 10.75 m wide and 7.3 m high. The materials of the floor, sidewalls, and ceiling are set as "concrete", which is a common material used for highway tunnels. The left portal of the tunnel is set as an air "supply" vent to provide longitudinal ventilation, and the other is set as "open." The "simple chemistry" combustion model uses N-Heptane fuel [29]. Based on the fire scale for different types and numbers of vehicles published by PIARC [30], the fire scale for full truck fires (30 MW) is chosen as HRR in consideration of the worst-case scenario. The fire source is 2.6 m in height, which is the height of a normal truck. The ambient pressure was set as 101.325 kPa, and the ambient temperature was set as $20 \,^{\circ}\text{C}$. The gravity is considered to be $9.81 \, \text{m/s}^2$. The quality of the fuel was ignored based on the methods of previous studies, and the simulation time was set as $450 \, \text{s}$. The determination of the curvature radius for the tunnel model relied on both existing tunnel data and compliance with minimum curvature radii mandated by applicable codes [21,22] corresponding to specific design speeds. In addition, in a straight tunnel, the radius of curvature is ∞ .

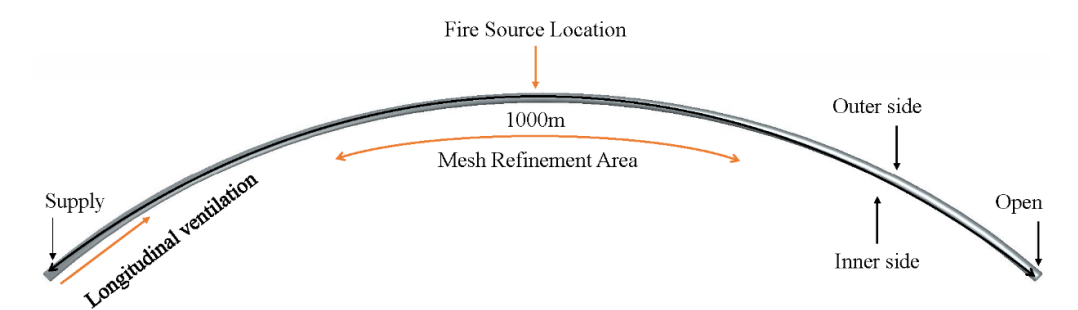


Figure 1. Tunnel fire model.

2.3. Critical Velocity

For further research into smoke movement characteristics and their impact on personal evacuation, longitudinal ventilation velocity must be taken into consideration. In practical fire scenarios, longitudinal ventilation velocity has a significant influence on the diffusion of fire smoke. However, natural wind in tunnels exhibits frequent fluctuations with constantly changing wind direction and velocity. Notably, mechanical ventilation measures implemented within the tunnel were not accounted for in this calculation.

According to the existing research, Equation (1) is chosen to calculate critical velocity [22].

When
$$\dot{Q}/\rho_a C_p T_a \sqrt{g} H^{5/2} \le 0.15 (H/W)^{-1/4}$$
,

$$u/\sqrt{gH} = 0.81 \left(\dot{Q}/\rho_a C_p T_a \sqrt{g} H^{5/2} \right)^{1/3} (H/W)^{1/12} e^{-L_b/18.5H}, \tag{1a}$$

When
$$\dot{Q}/\rho_a C_p T_a \sqrt{g} H^{5/2} > 0.15 (H/W)^{-1/4}$$
,

$$u/\sqrt{gH} = 0.43e^{-L_b/18.5H} \tag{1b}$$

where ρ_a is the ambient density; C_p is the heat capacity; g is gravitational acceleration, H is the tunnel height; L_b is the back-layering length, where $L_b = 0$ defines critical velocity; T_{α} is the ambient gas temperature; u is the longitudinal velocity; and W is the tunnel width.

Appl. Sci. 2024, 14, 6339 4 of 18

As shown in Equation (1), ambient density, ambient gas temperature, and heat capacity change as altitude increase. As a result, the maximum critical velocity of 3.56 m/s is chosen to design the simulations.

Based on the existing tunnel operating period data [31,32], the control wind velocity of tunnel longitudinal ventilation varies from 2.0 m/s (the maximum natural longitudinal ventilation velocity) to 8.0 m/s (the maximum control longitudinal ventilation velocity). When a fire occurs, the tunnel wind velocity should be a little greater than the critical wind velocity. According to the national code, the radius of the curvature of simulations was chosen as the minimum turning radii at different speed [33].

Existing studies [6,7,15,34,35] show that the curvature of a tunnel will affect the critical velocity of a tunnel fire. Therefore, 4 m/s was selected as the critical velocity in this paper. Subsequent simulation results also show that tunnel curvature has an effect on the critical velocity.

A general velocity group (the longitudinal ventilation velocity is 2 m/s; tests 1, 3, 5, 7, 9, 11, 13, 15, and 17) and a critical velocity group (the longitudinal ventilation velocity is 4 m/s; tests 2, 4, 6, 8, 10, 12, 14, 16, and 18) were set to study fire smoke movement characteristics under natural longitudinal ventilation velocity and control longitudinal ventilation velocity in the fire scenario. Except longitudinal ventilation, no other mechanical ventilation measures were taken into account in the simulation. All the tests are shown in Table 1.

No.	Radius of Curvature, m	Longitudinal Ventilation Velocity, m/s
1, 2	∞	2, 4
3, 4	250	2, 4
5, 6	400	2, 4
7,8	600	2, 4
9, 10	800	2, 4
11, 12	1000	2, 4
13, 14	1200	2, 4
15, 16	1500	2, 4
17, 18	2000	2, 4

2.4. Grid Size

Existing studies have shown that grid size has a great influence on the accuracy of simulation results, and mesh size has a strong relationship with the fire characteristic diameter D^* . When the fire characteristic diameter D^* is between 4 and 16 times the grid size, the simulation results can reflect the real situation more accurately [24] The calculation method of D^* is as follows:

$$D^* = \left(\dot{Q}/\rho_{\infty}c_p T_{\infty}\sqrt{g}\right)^{2/5},\tag{2}$$

where D^* is the fire characteristic diameter, Q is the HRR, ρ_{∞} is the air density, c_p is the specific heat capacity of air, T_{∞} is the ambient temperature, and g is the gravity acceleration. As shown in Equation (1), the fire characteristic diameter will increase when the ambient pressure decreases.

As a result, the suitable grid size for the present 30 MW fire ranged between 0.233 m and 0.94 m. The simulation results for the case of curvature radius of 800 m and with ventilation of 2 m/s (the same as test 9) at 150 s were compared using five different grid sizes of 0.25 m, 0.3 m, 0.4 m, 0.5 m, 0.6 m, and 0.9 m, as shown in Figure 2. It is seen that as the grid size decreases, the temperature discrepancy becomes insignificant. Except for the gird sizes of 0.6 m and 0.9 m, the vertical temperatures near the tunnel ceiling from other grid sizes were similar. When the grid size was no more than 0.5 m, the accuracy of the simulations with smaller grid sizes did not improve significantly but required more

Appl. Sci. 2024, 14, 6339 5 of 18

simulation time. Therefore, the grid size was finally determined as 0.5 m. Considering that the flow fields near the fire source were more complex, the grid size in the zone within a 200 m radius surrounding the fire source was refined as 0.25 m, and the grid sizes in the rest zones were set as 0.5 m.

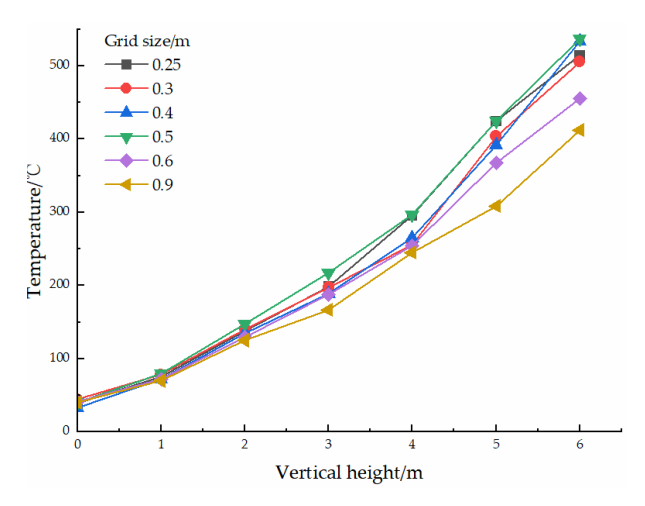


Figure 2. Vertical temperature distribution 10 m downstream of the fire source under different grid sizes for a curvature radius of 800 m and a ventilation of 2 m/s at 150 s.

2.5. Verification of Numerical Simulation Reliability

To verify the simulation results, we attempted to compare them with the experimental results. Three full-scale tunnel fire experiments were conducted in a highspeed railway tunnel by Pan et al. [36]. The flame height, longitudinal distribution of smoke temperature, and longitudinal smoke velocity were studied. In this research, the ambient temperature was $20.7~^{\circ}$ C. Test 3 in this paper had a longitudinal ventilation velocity of 0 m/s, a fire area of $2.0~\text{m}^2$, and a fire scale of 4 rectangular oil trays filled with 92-octane gasoline, each with a thickness of 2 cm. Based on the full-scale tunnel fire experiment, the results were compared with simulation results in this work for a special test, as shown in Figure 3. This figure shows that the FDS predictions match the experimental results well.

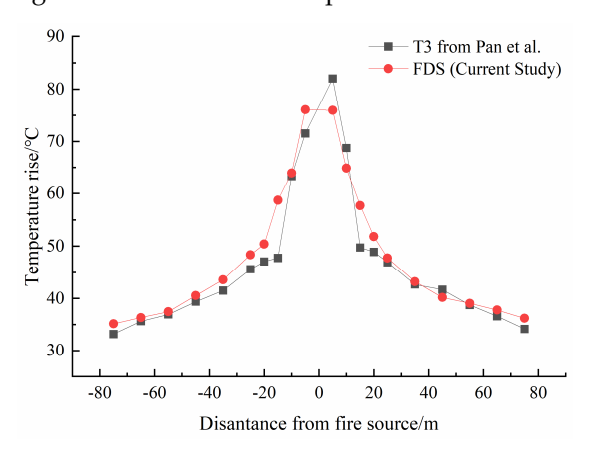


Figure 3. Comparison of the temperature rise in T6 from Pan's experiment [36] and the simulation results of this work.

The experimental results for the longitudinal distribution of the maximum temperature rise in fire smoke in a tunnel at 120 s from [36] are compared with the numerical results, as shown in Figure 3. At each data point, the simulation results of FDS were in good overall agreement with the experimental values, typically within a 5% deviation. However, an error margin of 8% was observed at a distance of 5 m from the fire source. These discrepancies become negligible away from the fire source because of complex turbulent and heat transfer phenomena that occur near the fire source. These differences are mainly because the wind

Appl. Sci. 2024, 14, 6339 6 of 18

velocity in the FDS model was set as 0, which continuously varied during Pan's experiment. Overall, the comparative results prove that the FDS predictions match the experimental results well.

2.6. Determination of the Location of the Most Hazardous Fire Source

In a single tunnel for subtended traffic, ignoring the urgent parking strip, the smoke distribution caused by a fire source vehicle located in either the inner or outer lane will exhibit variations. A model with a curvature radius of 400 m and ventilation wind speed of 4 m/s was established for verification. When the fire source is in the outer lane or the inner lane, the temperature distribution on the ceiling, the inner wall, the outer wall, and the middle line at the 2 m characteristic height of the tunnel at 300 s are shown in Figure 4. Regardless of the location of the fire source, the temperature distribution on the tunnel ceiling remains consistent. However, when the fire source is positioned on the inner side of the tunnel bend, there is an extended range of high-temperature (over 60 $^{\circ}$ C) areas at human eye characteristic height compared with when it is located on the outer side. Consequently, it can be concluded that positioning the fire source vehicle on the inner tunnel lane represents the worst-case scenario. The fire source is consistently positioned at this location in all subsequent calculations.

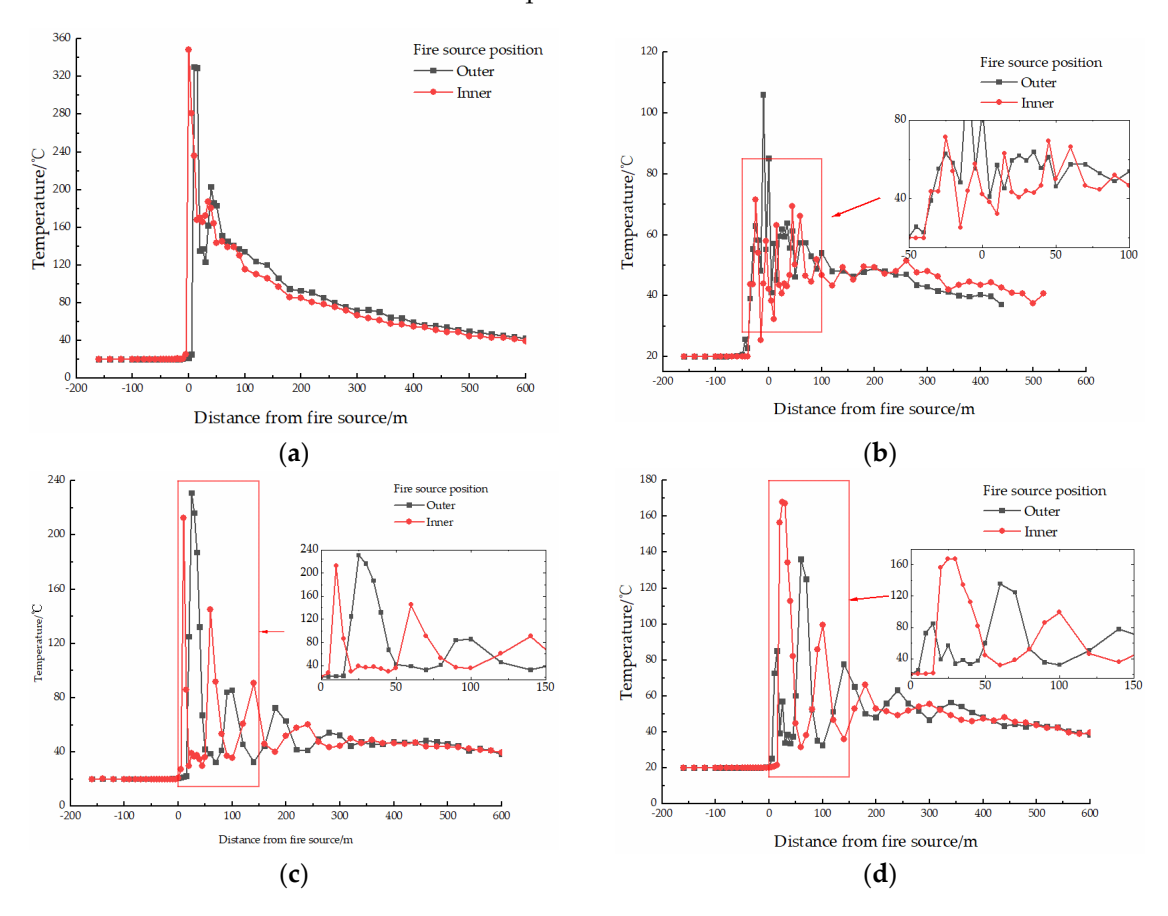


Figure 4. Comparison of the ceiling temperature and characteristic height of different fire source positions. (a) Temperature at the tunnel ceiling; (b) Temperature of the center line at 2 m height; (c) Temperature of the inner side at 2 m height; (d) Temperature of the outer side at 2 m height.

3. Results

3.1. Safety Standard

In order to investigate the distribution characteristics of fire smoke and their impact on personal evacuation, this study focuses on the one-dimensional spread of smoke at the characteristic height of human eyes. The safety standard for the smoke temperature at the Appl. Sci. 2024, 14, 6339 7 of 18

characteristic height was set at 60 $^{\circ}$ C, in accordance with national codes [37]. Similarly, a visibility of 10 m and a CO concentration of 400 ppm was set as the standard for visibility and CO concentration. The characteristic height was defined as 2 m in this study.

3.2. Comparison of the Smoke Distribution in Different Sides of the Tunnel

To further analyze the characteristics of the smoke distribution in the tunnel, the simulations were categorized into two groups as follows: Group A and Group B. Group A comprised four different simulations with curvature radii of 250 m, 400 m, 600 m, and 800 m, whereas Group B consisted of four simulations with curvature radii of 1000 m, 1200 m, 1500 m, and 2000 m. Both Group A and Group B were compared to straight tunnels to assess the impact of tunnel curvature. The one-dimensional distribution characteristics of fire smoke at the characteristic height at 360 s are analyzed in this paper.

3.2.1. Temperature

In previous studies, the fire source location has predominantly been assumed to be at the centerline of the tunnel, resulting in symmetrical horizontal and longitudinal temperature distributions. However, considering real scenarios, when a vehicle catches fire in a tunnel, it is more likely that the fire source vehicle will be positioned on one side of the tunnel.

Figure 5 shows the longitudinal temperature distribution at the characteristic height for the critical velocity group at 360 s. In this scenario, the rapid rise in temperature within the fire source area is attributed to the generation of high-temperature flames and smoke. This phenomenon is represented by the initial peak on the temperature distribution figure at the inner side of the tunnel. Subsequently, propelled by longitudinal ventilation, the high-temperature smoke propagates forward. However, because of the bending of the tunnel, it collides with and rebounds off the outer wall, resulting in a distinct peak region on its surface. The variation in the curvature of the tunnel leads to the difference in the location of the outer side temperature peak. Consequently, multiple peaks are observed as the hightemperature smoke repeatedly interacts between the inner and outer sides. As one moves away from the fire source, the fluctuations in temperature in the centerline of the tunnel become smaller and gradually downward. The location and height of the temperature peak of Group A (tests 4, 6, 8, and 10) significantly differ from those observed in the straight tunnel (test 2). This discrepancy can be attributed to the influence of the curved tunnel on the initial impact position of high-temperature smoke flow under longitudinal ventilation conditions, resulting in variations in the subsequent temperature distributions.

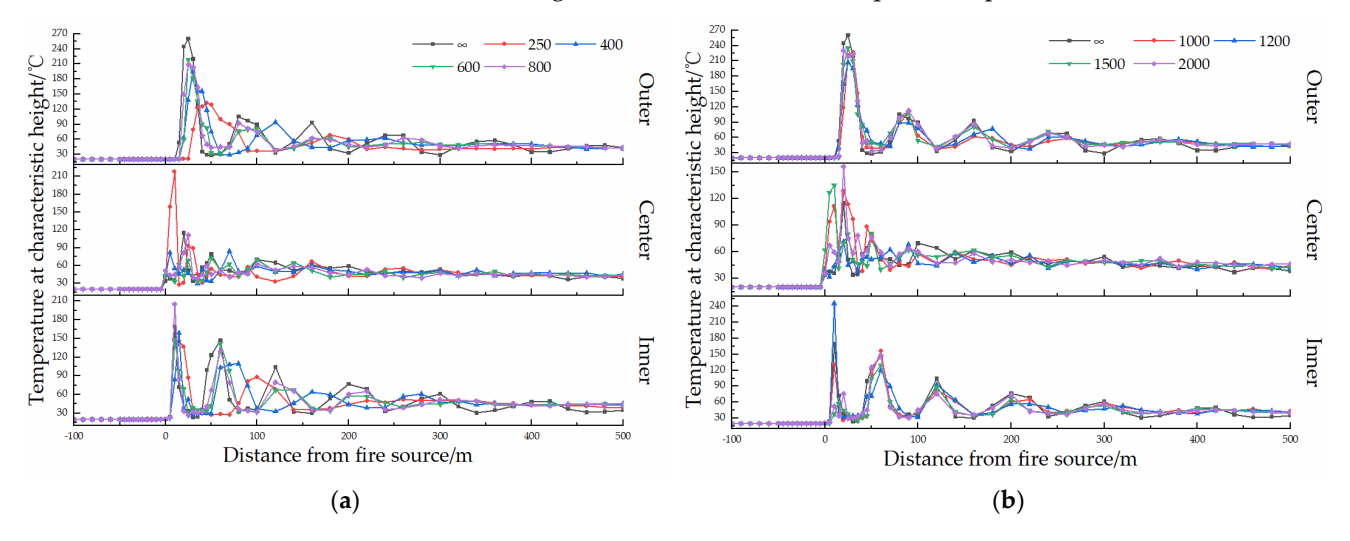


Figure 5. Variation in longitudinal temperature at the characteristic height of the critical velocity group. (a) Comparison of temperature on different sides of the tunnel for Group A. (b) Comparison of temperature on different sides of the tunnel for Group B.

Appl. Sci. 2024, 14, 6339 8 of 18

For Group B (tests 12, 14, 16, and 18), the longitudinal temperature distribution on the tunnel's inner side, outer side, and centerline closely resembles that of the straight tunnel (test 2). However, notable disparities arise in terms of peak temperature values between the inner side and outer side of the tunnel at the corresponding distance from the fire source. The numerical comparisons reveal significant differences in both the temperature distribution and peak temperatures between the tunnel curvature radius of 1000 m and 1200 m with a straight tunnel. Conversely, when the tunnel curvature radius is set as 1500 m and 2000 m, the temperature distribution and peak temperatures are relatively the same as those observed in the straight tunnel.

However, when the tunnel ventilation velocity is below the critical velocity, the longitudinal temperature distribution exhibits distinct variations, as shown in Figure 6. Under such circumstances, the driving force of longitudinal ventilation for high-temperature smoke within the tunnel becomes insufficient, resulting in its predominant distribution along the longitudinal ventilation of the tunnel. Nevertheless, the curved wall still exerts a certain inhibitory effect on smoke spread. This is primarily manifested by a consistent temperature distribution along the centerline of the tunnel in different simulations without significant differences observed. The primary distinction between the inner and outer sides of the tunnel lies in the maximum temperature within the core area of the fire source. However, beyond this core area, the smoke enters a one-dimensional longitudinal propagation stage.

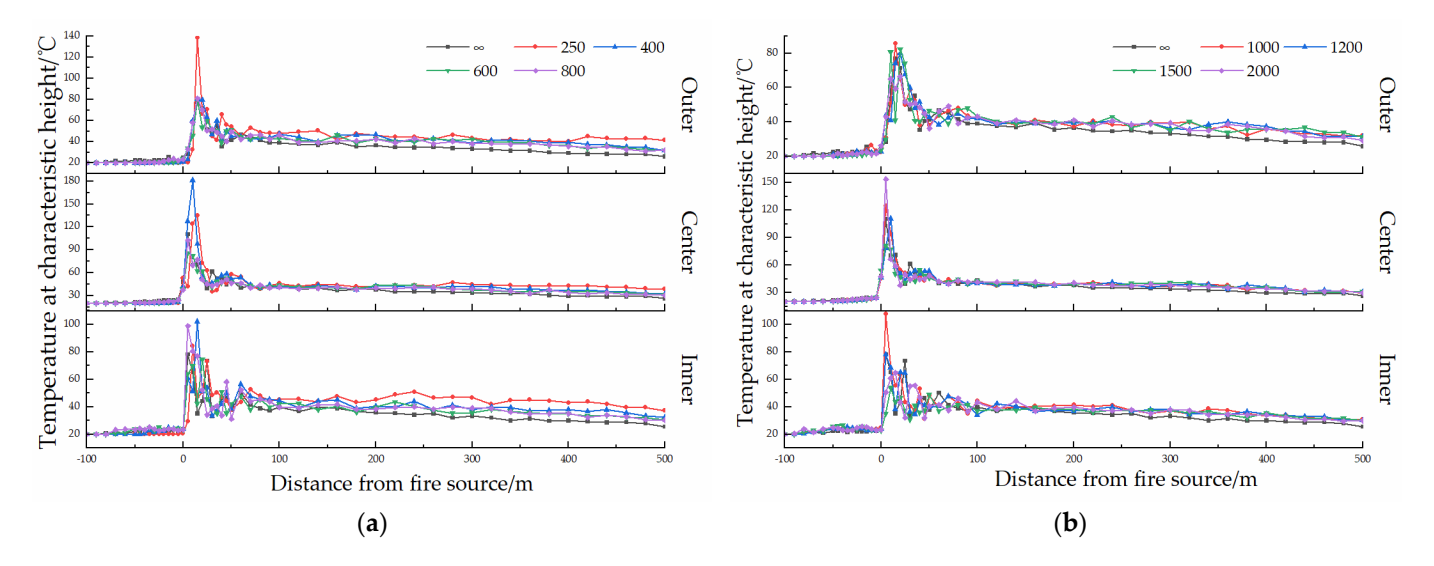


Figure 6. Variation in longitudinal temperature at the characteristic height of the general velocity group. (a) Comparison of temperature on different sides of the tunnel for Group A. (b) Comparison of temperature on different sides of the tunnel for Group B.

3.2.2. Visibility

Figure 7 shows the longitudinal variation in the visibility of the critical velocity group at the characteristic height at 360 s. Initially, during the early stages of the fire, smoke primarily accumulates in the tunnel ceiling because of the heat generated by the fire source. This accumulation has minimal impact on visibility at the characteristic height, as there are no significant alterations in temperature or smoke concentration. However, as the fire progresses, smoke diffuses longitudinally throughout the tunnel. The distribution of human visibility corresponds to the longitudinal distribution of temperature and reflects alternating zones of fire smoke caused by the high-temperature smoke and flame between the inner and outer sides of the tunnel.

Appl. Sci. 2024, 14, 6339 9 of 18

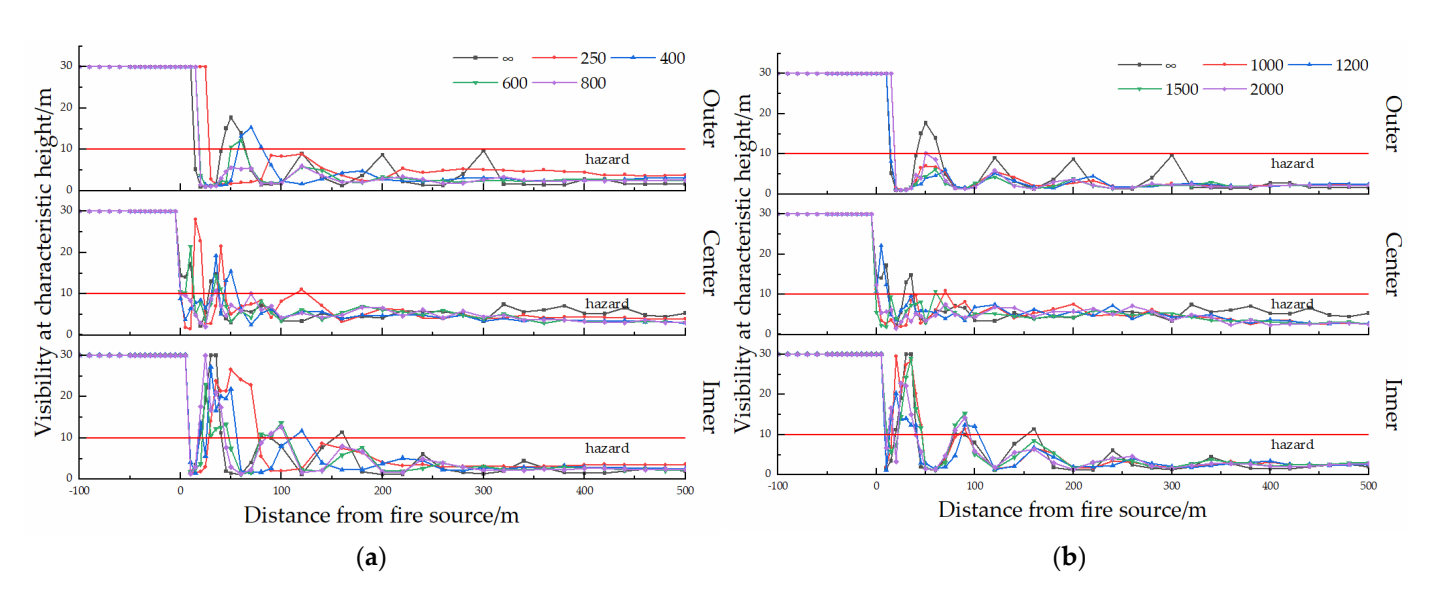


Figure 7. Variation in longitudinal visibility at the characteristic height of the general velocity group. (a) Comparison of visibility on different sides of the tunnel for Group A. (b) Comparison of visibility on different sides of the tunnel for Group B.

Group B (tests 12, 14, 16, and 18) exhibits a similar trend in visibility distribution compared to that observed in a straight tunnel (test 2). The main difference is that the visibility at 50 m away from the fire source of the straight tunnel remained in the safe range, while group B is at the peak of visibility but still within the hazardous range. For group A (tests 4, 6, 8, and 10), the peak position and peak height of its visibility are significantly different from those of the straight tunnel. However, when the distance from the fire source exceeds 150 m, the visibility is lower than 10 m in all simulations, which means there remains no difference in personal evacuation. However, when the tunnel ventilation velocity is below the critical velocity, as shown in Figure 8, there is a significant disparity in the longitudinal visibility distribution within the general velocity group. Longitudinal ventilation is insufficient to drive the high-temperature smoke in the tunnel under such simulations. Beyond a distance of 50 m away from the fire source, human visibility for all simulations falls into the dangerous range. Noticeable smoke back-layering occurs. In Group A, variations in tunnel curvature greatly influence the impact of smoke backlayering length on human visibility upstream of the fire source. Because of obstruction by the inner sidewall of the tunnel, the smoke temperature decreases more rapidly compared with that on the outer side, resulting in a rapid visibility decrease at the characteristic height. Nevertheless, human visibility remains within safe limits on the outer side of the tunnel; this remains true for Group B as well. Although tests 16 and 18 exhibit similar patterns of smoke and temperature distribution as those observed in a straight tunnel within Group B, there are still notable differences in visibility upstream of the fire source and at the centerline.

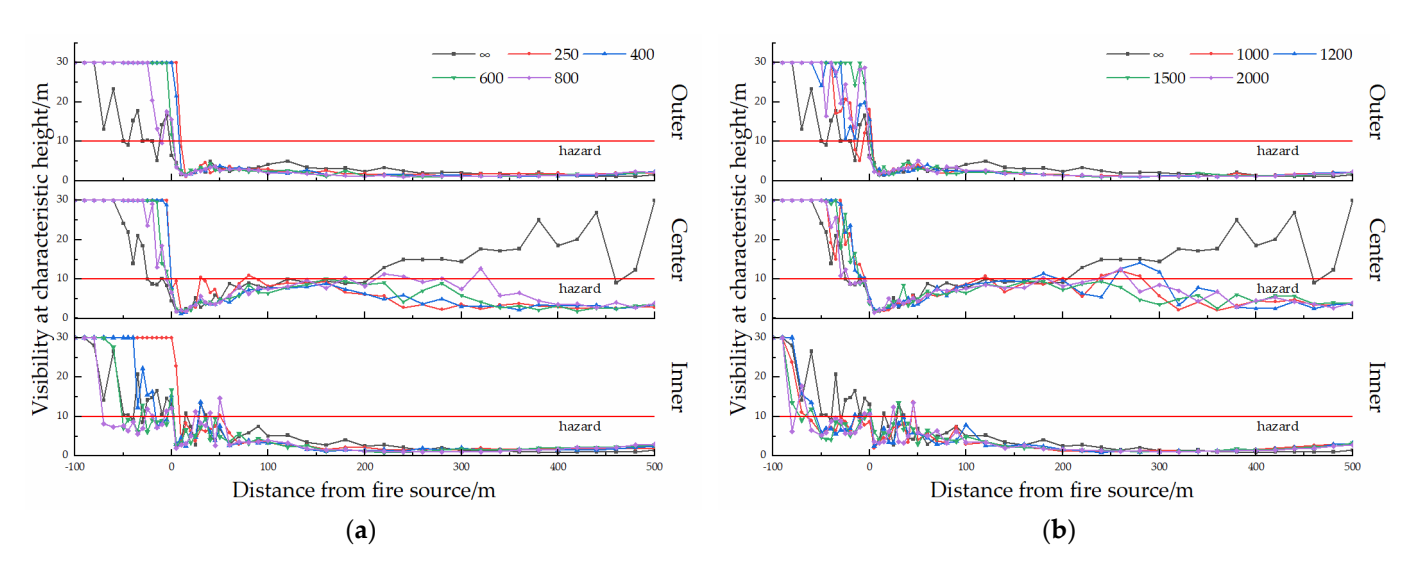


Figure 8. Variation in longitudinal visibility at the characteristic height of the general velocity group. (a) Comparison of temperature on different sides of the tunnel for Group A. (b) Comparison of temperature on different sides of the tunnel for Group B.

3.2.3. CO Concentration

The variation in the longitudinal CO concentration at the characteristic height of the critical velocity group and the general velocity group in the 360 s tunnel is shown in Figures 9 and 10. It is observed that tunnels with curved structures exhibit a more pronounced increase in CO concentration within the core area of the fire source. This suggests that compared with straight tunnels, the incomplete combustion of combustible materials is exacerbated in curved tunnels during fire events. Toxic gases like CO, predominantly found in fire smoke, pose significant risks to personal evacuation. Incomplete combustion occurs at various stages of a fire. However, it takes some time for CO concentration to reach a hazardous level.

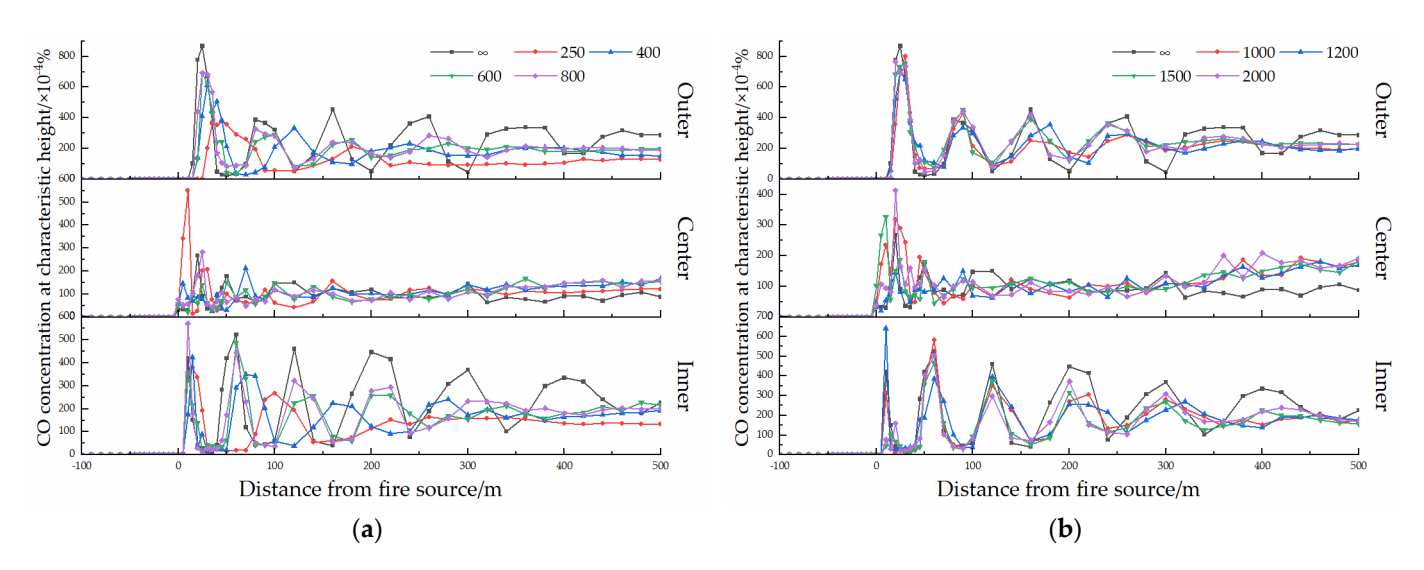


Figure 9. Variation in longitudinal CO concentration at the characteristic height of the critical velocity group. (a) Comparison of CO concentration on different sides of the tunnel for Group A. (b) Comparison of CO concentration on different sides of the tunnel for Group B.

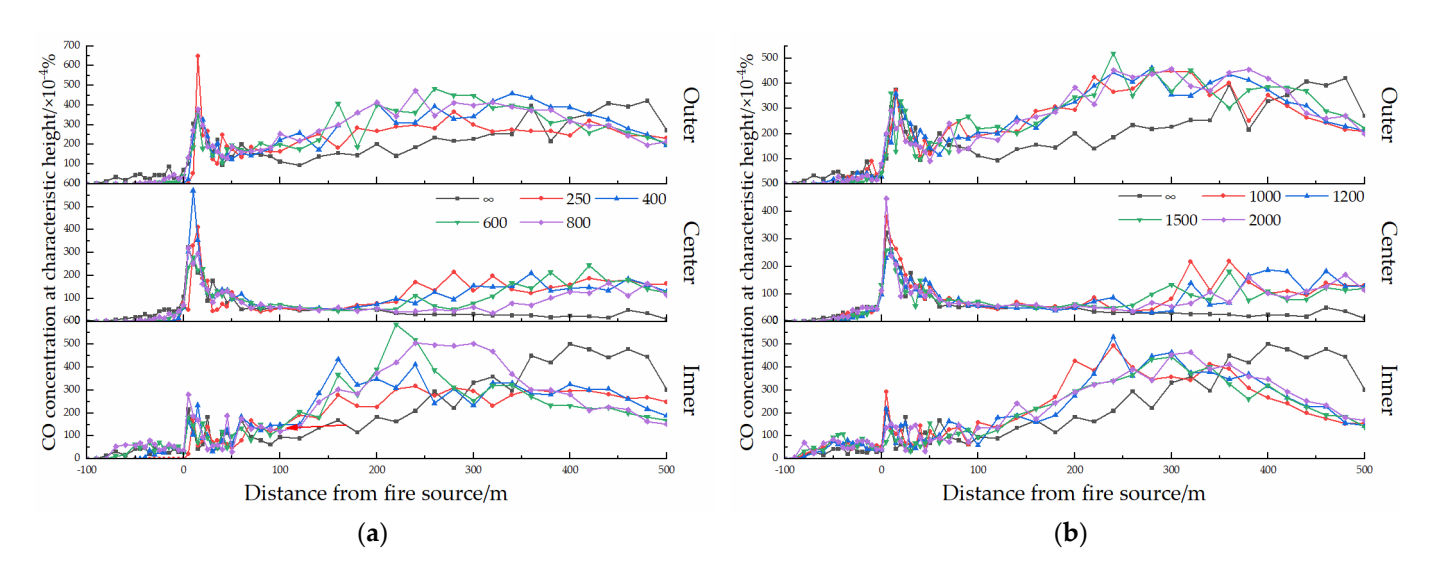


Figure 10. Variation in longitudinal CO concentration at the characteristic height of the general velocity group. (a) Comparison of CO concentration on different sides of the tunnel for Group A. (b) Comparison of CO concentration on different sides of the tunnel for Group B.

As shown in Figure 9, the longitudinal ventilation in the critical velocity group effectively suppresses smoke back-layering. However, because of the unique tunnel structure, high-temperature smoke does not directly disperse outward along the tunnel but instead transports between the lateral walls. The longitudinal diffusion of CO is generally consistent with temperature and visibility trends. Except for the fire source core area, CO concentration remains below hazardous levels. Nevertheless, a comparison between Group A and Group B reveals that as the radius of curvature increases, both sides of the tunnel and its centerline experience decreased CO concentrations. Furthermore, the longitudinal distribution of CO concentration on the outer and inner sides gradually approaches that observed in straight tunnels. However, higher CO concentrations persist at the centerline compared with those found in straight tunnels.

However, when the longitudinal ventilation velocity is below the critical velocity, the longitudinal distribution pattern of CO concentration in curved tunnels differs significantly from that observed in straight tunnels, as shown in Figure 10. The CO concentration in curved tunnels with different radii of curvature at the outer side and the centerline of the tunnel upstream of the fire source remains consistent with that in straight tunnels, indicating a low level. However, because of structural influences on airflow patterns, there is a notably higher CO concentration on the inner side of curved tunnels. In terms of core areas near the fire source, CO concentrations are generally comparable between curved and straight tunnels. Nevertheless, within a range of 100-350 m away from the fire source, both the inner and outer sides exhibit higher CO concentrations compared with those found in straight tunnels. However, CO concentration levels remain similar to those observed along the centerline in straight tunnels. Beyond 350 m from the fire source, there is a significant increase in CO concentration along the centerline of curved tunnels relative to that seen in straight tunnels. The downward trend observed for CO concentrations on both the inner and outer sides gradually causes them to become lower than those measured within straight tunnels.

The tunnel set in the simulations comprises an arched ceiling, through which CO is transported along with the flue gas. Subsequently, CO ascends to the tunnel ceiling before descending towards both sides. The spatial distribution of CO is deemed to be influenced by the radius of curvature of the tunnel.

3.3. Comprehensive Analysis of the Altitude Effect and Longitudinal Ventilation

The longitudinal distribution patterns of temperature, visibility, and CO concentration collectively reflect the distribution characteristics of fire smoke in the tunnel. Specifically,

when the longitudinal ventilation velocity in the tunnel exceeds the critical velocity, hightemperature flames and smoke generated by the offset fire source rapidly propagate along the tunnel direction under the influence of longitudinal ventilation. However, this propagation does not align perfectly with the longitudinal ventilation direction but exhibits a certain deviation. Subsequently, the high-temperature smoke impacts and rebounds off from the outer wall of the tunnel. This phenomenon is manifested as the first peak in temperature and CO concentration as well as a low visibility zone on the inner side of the tunnel. Afterward, there is an alternating reflection and cooling process between both the inner and outer walls for high-temperature smoke. The primary distinction observed in tunnels with different curvatures lies in the positions and values of the numerical peaks. Nevertheless, when compared with straight tunnels, if the longitudinal ventilation velocity falls below the critical velocity within a curved tunnel, temperature, visibility, and CO concentration exhibit similar patterns downstream from 0 m to 100 m relative to that emitted by the fire source. The temperature, visibility, and CO concentration decrease with increasing distance from said source. However, the upstream region experiences significant differences because of the smoke back-layering caused by tunnel curvature effects. Moreover, tunnel curvature significantly contributes to increased CO concentration within regions located 100-350 m downstream of the fire source.

3.4. Impact on Personal Evacuation

3.4.1. Impact on Available Safe Egress Time

Based on the distribution of temperature, visibility, and CO concentration, the available safe egress time (ASET) was determined when any factor reached a hazardous level. In the case of a tunnel fire, personal safety is primarily threatened by the following three factors: the temperature rise in the fire source area, the decrease in visibility due to smoke diffusion, and the dispersion of toxic gases. These three factors combine to the hazardous range gradually. A comparative analysis reveals that temperature is the key hazardous factor contributing to disaster in the core area of a tunnel fire. At approximately 120 s, temperatures enter hazardous levels within the core area. When a fire occurs in a highway tunnel, the longitudinal wind velocity would be accelerated over critical velocity [21]. Therefore, the following analysis is based on the results of the critical velocity group.

As discussed above, when a fire occurs in a curved tunnel, the distribution of high-temperature smoke on the inner and outer sides of the tunnel presents a certain difference. Figure 11 shows the differences between the ASET on the inside and outside of the tunnel. From left to right and from top to bottom, the corresponding curvature radii of each tunnel are 250 m, 400 m, 600 m, 800 m, 1000 m, 1200 m, 1500 m, and 2000 m.

As shown in Figure 11, regardless of the radius of curvature, the inner side of the tunnel has more available safe egress time than the outer side within the core area of the fire and an area distance of 150 m from the fire source. Within a distance range of 75–150 m from the fire source, as previously mentioned, when high-temperature smoke impacts the outer tunnel wall and reflects towards the inner wall, it gives rise to a localized weak zone of high-temperature smoke through successive reflections. However, it is important to note that the weak region of the temperature distribution near the core zone of the fire source, as depicted in Section 3.2.1 when high-temperature smoke impacts the opposite side of the tunnel, will still transition into the hazardous range of human visibility at an early stage.

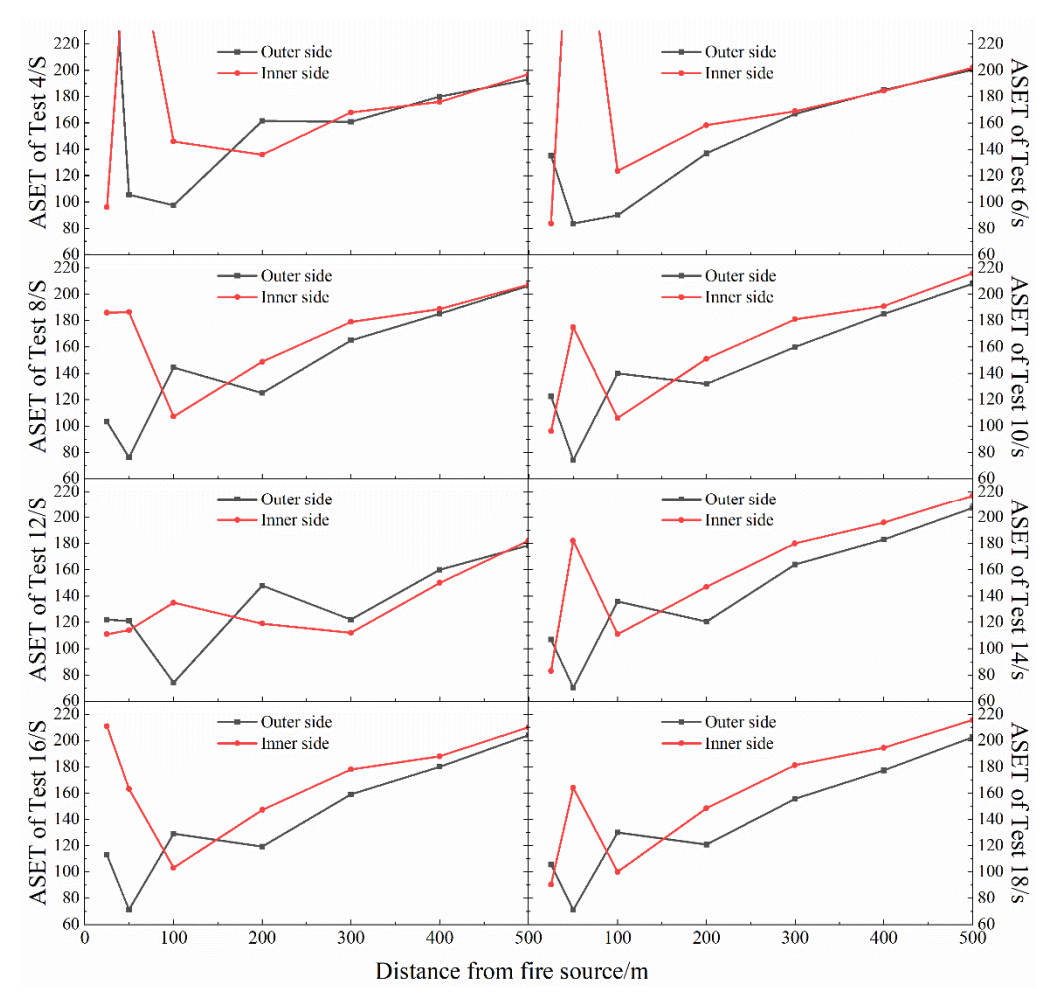


Figure 11. ASET of tunnels with different curvature radii at different distances from the fire source.

3.4.2. Position of an Adit for People Passing

Based on the above results, when designing personal escape routes for curved tunnels, it is recommended to strategically position an adit for people passing on the inner side of the tunnel to maximize the available safe egress time.

3.4.3. Position of the Adit for People Passing

The existing investigations and analyses suggest that the response to a fire can generally be categorized into three primary stages as follows: fire detection, confirmation of fire occurrence, and evacuation actions [38]. To ensure the safe evacuation of all persons, particularly in hazardous situations, it is imperative to establish adequate spacing of adits for people passing so that individuals can safely move from upstream and downstream areas of the fire source. The maximum permissible distance should be defined as the distance that people can safely evacuate within the required safe egress time (RSET). The RSET is

$$REST = T_d + T_{pre} + T_t, (3)$$

where T_d is the alarm time; T_{pre} is the pre-moving time for personal evacuation; and T_t is the personal evacuation time.

The smoke detectors used in actual engineering can detect fires of 100 kW. The fire alarm start time is calculated based on the t^2 fire model in this research. Typically, the development law of fires in the initial stage is as follows:

$$Q_f = \alpha t^2 \tag{4}$$

Appl. Sci. 2024, 14, 6339 14 of 18

where t is the time of fire occurrence; Q_f is HRR, which is set as 100 kW in the calculation of alarm time; and α is the fire growth coefficient, which is set as 0.187 kW/s² in this study. Therefore, the alarm time of the fire detection system can be determined as follows:

$$T_d = sqrt(Q_f/\alpha) = sqrt(100/0.187) \approx 23.1 \text{ s}$$
 (5)

The time interval between the receipt of the fire alarm and the initiation of evacuation measures, known as the pre-action time or personal evacuation response time, is crucial in fire emergencies. Determining the pre-action time primarily depends on factors such as building type and characteristics associated with occupant safety. The existing research data [39–42] show that the pre-moving time for personal evacuation ranges from 30 s to 210 s. In this study, a pre-action time of 90 s was observed.

Currently, no study has indicated any influence of the curvature radius on personal evacuation speed or their choices in a curved tunnel. Therefore, the personal evacuation time T_t is assumed to be consistent between curved and straight tunnels. This issue is not further discussed in this paper.

Figure 12 shows the temperature distribution in the tunnel with a curvature radius of 400 m within 200 m from the fire source. From left to right, the temperature distributions are at 83.1 s, 113.1 s, 143.1 s, and 173.1 s. Based on the set alarm time of 23.1 s and the pre-moving time for a personal evacuation of 90 s, people will start to evacuate at 113.1 s, and the temperature distribution in the tunnel at this time is shown in Figure 12 b.

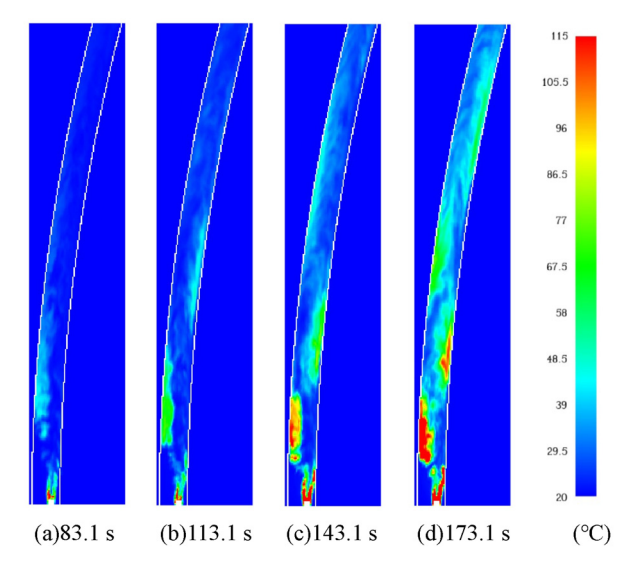


Figure 12. Temperature distribution of the tunnel within 210 m from the fire source at different times.

At this time, as discussed before, the high-temperature smoke hits the outer wall of the tunnel for the first time, which leads to the green area on the outer side. The green area means that the temperature within this area approaches 60 °C, which is not suitable for people to pass through. In general, during evacuation procedures, individuals should disperse along the pedestrian lane on both sides of the traffic lanes. However, the hazardous zone formed in the outer side of the tunnel, which means people should evacuate along the inner side of the tunnel.

As shown in Figure 12c, the second hit of the high-temperature smoke appeared at 143.1 s. The presence of a second high-temperature zone within the tunnel renders the inner side unsuitable for evacuation, necessitating the evacuation route to be redirected along the outer side of the tunnel.

However, the feasibility of such back-and-forth movement between the inner and outer sides of the tunnel is compromised for individuals trapped in a fire.

Therefore, in the case of fires that occur in curved tunnels, it is recommended that persons located at the core area of the fire source promptly evacuate along the center line of

the tunnel. Once they have moved beyond a distance of 100 m from the fire source, they should continue their evacuation along the inner wall of the tunnel and exit through an adit for people passing.

Meanwhile, the comparison shown in Figure 12 also suggests that if the pre-moving time for personal evacuation can be reduced to 60 s, the existing research on personal evacuation speed [21,43–45] indicates individuals will be capable of evacuating from the core area of fire source before a high-temperature zone forms. Beyond the core area of the fire source, the primary hazardous index of personal evacuation shifts from temperature to visibility.

4. Discussion

This research into smoke diffusion in curved highway tunnel fires revealed distinct patterns of fire characteristics at human eye height. Compared with straight tunnels, the movement of smoke in curved tunnels exhibits different patterns. The propagation of fire smoke can be categorized into the following two stages: the fire development stage and the one-dimensional longitudinal spreading stage [46]. During the fire development stage, high-temperature smoke generated directly by the fire source undergoes repeated collisions between the inner and outer sidewalls of the tunnel. Consequently, this process results in multiple high-temperature zones between the inner and outer sides. Additionally, CO, which significantly impacts personal evacuation because of the incomplete combustion of the fire source, also exhibits alternating peaks between the inner and outer sides as it spreads with high-temperature smoke. However, subsequent smoke diffusion resembles that in a straight tunnel where visibility is less influenced by smoke temperature due to transmission characteristics but more affected by smoke concentration. Following the initiation of one-dimensional longitudinal smoke diffusion, there is no discernible variation in temperature or visibility across different locations within the tunnel. Nevertheless, the distribution of CO does not entirely align with smoke diffusion. Within high-temperature smoke, distinct zones of alternating CO concentration peaks persist on both the inner and outer side walls during the one-dimensional propagation phase.

The results on the distribution of temperature agree well with previous studies [4,14,18]. However, it must be pointed out that we further considered two critical indicators, i.e., CO concentration and human visual acuity, when comparing our results to those of older studies. Additionally, the selection of the tunnel curvature radius was not constrained to a minimum value of 2500 m [16]. Based on practical engineering, the longitudinal ventilation velocity was introduced into the simulations to consider the smoke propagation pattern in the actual fire scenario. The results extended beyond the scope of smoke control measures to encompass considerations for the selection of personal evacuation strategies.

The limitations of our study should be acknowledged when interpreting these findings. Firstly, it is important to emphasize that the temperature distribution results have been validated by enough experiments [11,15], ensuring the accuracy of our findings. The distribution of human visibility has also been rigorously substantiated. Nonetheless, there remains a need for experimental verification regarding the distribution pattern of CO concentration in curved highway tunnels. In current numerical simulations, the heat release rate of the fire source is consistently assumed to be a super-fast fire. However, the heat release rate of the fire source exhibits a discernible trend of gradual increase. Moreover, our selection of simulations has limitations. As no completely flat tunnels are unaffected by altitude in actual engineering, our study remains constrained. Variations in air density, humidity, and oxygen content of the tunnel location will also impact the results. Despite its preliminary character, our study clearly indicates the influence of different tunnel curvature radii on fire smoke dispersion and personal evacuation.

One important future direction is to explore the combined effects of multiple influencing factors. For example, investigating the impact of altitude effects and chimney effects on the diffusion pattern of fire smoke in a curved tunnel can help elucidate their potential to either enhance or suppress smoke distribution. Another important future

direction is a transition curve section between the straight area and the curved area. The influence of the continuously changing curvature radius on smoke distribution is also worth further exploration.

A new personal evacuation strategy for curved highway tunnels can be derived from our findings. In straight tunnels, evacuation occurs along the sidewalks on both sides of the tunnel leading to an adit for people passing. However, in curved tunnels, to minimize harm and ensure safe evacuation, we recommended that individuals near the fire source initially evacuate along the centerline of the tunnel for a specific distance before transitioning to the side crosswalks.

5. Conclusions

To investigate the characteristics of temperature, CO concentration, and human eye visibility at characteristic heights, a series of numerical simulations were conducted considering the radius of curvature and longitudinal ventilation velocity. The impact on personal evacuation was designed based on the results. The major conclusions are as follows:

Under the influence of longitudinal ventilation, fire smoke in curved tunnels does not directly disperse toward the tunnel exit. Instead, smoke reflects between the inner and outer sidewalls of the tunnel. Consequently, multiple high-temperature zones are formed on both sides of the tunnel near the source of the fire. The location of high-temperature zones changes with variations in the tunnel curvature radius, resulting in different characteristics of smoke distribution within the tunnel.

When the radius of curvature of the tunnel is less than 1000 m, there is a more pronounced disparity in smoke distribution characteristics between curved and straight tunnels. As the radius of curvature of the tunnel exceeds 1000 m, smoke distribution within curved tunnels gradually aligns with that within straight tunnels.

Because of the distinctive smoke distribution characteristics in curved tunnels, a comparison of fire source locations reveals that when the fire source vehicle is positioned in the inner lane of the tunnel, it poses a higher risk for personal evacuation. Consequently, through an analysis and comparison of temperature, visibility, and CO concentration distribution on both the inner and outer side walls across different curvature radii of tunnel curves, it is determined that the adit for people passing should be located on the inner side of the tunnel.

For personal evacuation within the core area of the fire source, considering the impact of high-temperature smoke distribution characteristics resulting from longitudinal ventilation in curved tunnels, we recommend initially conducting evacuations along the tunnel's central line. Subsequently, individuals should be guided along the inner pedestrian lane toward the adit for people passing away from the core area of the fire source.

Author Contributions: Conceptualization, Y.C. and Z.L.; methodology, Y.C.; software, Y.C.; validation, Y.C.; formal analysis, Y.C.; investigation, Z.L.; resources, Z.L.; data curation, Y.C.; writing—original draft preparation, Y.C.; writing—review and editing, Z.L.; visualization, Y.C.; supervision, Z.L.; project administration, Z.L.; funding acquisition, Z.L. All authors have read and agreed to the published version of the manuscript.

Funding: This research was funded by the National Natural Science Foundation of China, grant number 41461016 and grant number 41761015.

Institutional Review Board Statement: Not applicable.

Informed Consent Statement: Not applicable.

Data Availability Statement: The original contributions presented in the study are included in the article, further inquiries can be directed to the corresponding author.

Conflicts of Interest: The authors declare no conflicts of interest.

References

1. Du, T.; Li, P.; Wang, Y.; Xue, X. Longitudinal decay of smoke temperature and front velocity in tunnel fires. *China Saf. Sci. J.* **2023**, 33, 140–145. [CrossRef]

- 2. Jiang, X.-P.; Chen, X.-G.; Guo, K. Study on critical velocity of lateral point smoke extraction tunnel fire. *China Saf. Sci. J.* **2021**, 31, 105–111. [CrossRef]
- 3. Zhao, Q.; Li, J.-M.; Xie, X.; Liu, W. Numerical Study on Smoke Diffusion and Smoke Control in Urban Underground Curved Tunnel. *J. Phys. Conf. Ser.* **2023**, 2445, 012003. [CrossRef]
- 4. Kashef, A.; Saber, H.H.; Gao, L. Optimization of Emergency Ventilation Strategies in a Roadway Tunnel. *Fire Technol.* **2016**, 47, 1019–1046. [CrossRef]
- 5. Wang, F. Research on Key Parameters of Operation Ventilation of Curved Highway Tunnel. Ph.D. Thesis, Southwest Jiaotong University, Chengdu, China, 2010. [CrossRef]
- 6. Wang, F.; Dong, G.-H.; Wang, M. Study on the Critical Air Velocity for Fire Smoke Control in a Curved Tunnel. *Mod. Tunn. Technol.* **2015**, 52, 84–89. [CrossRef]
- 7. Wang, F.; Wang, M.; Carvel, R.; Wang, Y. Numerical study on fire smoke movement and control in curved road tunnels. *Tunn. Undergr. Space Technol.* **2017**, *67*, 1–7. [CrossRef]
- 8. Caliendo, C.; Ciambelli, P.; De Guglielmo, M.L.; Meo, M.G.; Russo, P. Numerical simulation of different HGV fire scenarios in curved bi-directional road tunnels and safety evaluation. *Tunn. Undergr. Space Technol.* **2012**, *3133*, 50. [CrossRef]
- 9. Wu, C.; He, J.; Ni, T. Research on the smoke movement in small radius curvilinear tunnel fires. *Fire Sci. Technol.* **2014**, *33*, 37–40. [CrossRef]
- 10. Wang, F.; Wang, M.-N. A computational study on effects of fire location on smoke movement in a road tunnel. *Tunn. Undergr. Space Technol.* **2016**, *51*, 405–413. [CrossRef]
- 11. Zhong, M.-H.; Shi, C.-L.; He, L.; Shi, J.; Liu, C.; Tian, X. Smoke development in full-scale sloped long and large curved tunnel fires under natural ventilation. *Appl. Therm. Eng.* **2016**, *108*, 857–865. [CrossRef]
- 12. Zhang, S.; Yang, H.; Yao, Y.; Zhu, K.; Zhou, Y.; Shi, L.; Cheng, X. Numerical Investigation of Back-Layering Length and Critical Velocity in Curved Subway Tunnels with Different Turning Radius. *Fire Technol.* **2017**, *53*, 1765–1793. [CrossRef]
- 13. Pan, R.-L.; Zhu, G.-Q.; Liang, Z.-H.; Zhang, G.; Liu, H.; Zhou, X. Experimental study on the fire shape and maximum temperature beneath ceiling centerline in utility tunnel under the effect of curved sidewall. *Tunn. Undergr. Space Technol.* **2020**, *99*, 103304. [CrossRef]
- 14. Lu, K.-X.; Xia, K.-H.; Shi, C.; Yang, M.; Wang, J.; Ding, Y. Investigation on the Tunnel Curvature Effect upon the Ceiling Temperature of Tunnel Fires: A Numerical Simulation. *Fire Technol.* **2021**, *57*, 2839–2858. [CrossRef]
- 15. Xu, Z.-S.; Zhou, D.-M.; Tao, H.; Zhang, X.; Hu, W. Investigation of critical velocity in curved tunnel under the effects of different fire locations and turning radiuses. *Tunn. Undergr. Space Technol.* **2022**, *126*, 104553. [CrossRef]
- 16. Muhasilovic, M.; Deville, M.O. Tunnel-Curvature's Influence on the Propagation of the Consequences of Large-Scale Accidental Fire—A CFD-Investigation. *Turk. J. Eng. Environ. Sci.* **2013**, 31, 391–402. [CrossRef]
- 17. Lu, F. Simulation Research on Fire Smoke Control in Curved Highway Tunnel. Ph.D. Thesis, Harbin Institute of Technology, Harbin, China, 2017. [CrossRef]
- 18. Zhao, W.-F.; Lv, S.-J.; Xu, H. Smoke movement characteristics of fire in small curvature radius tunnel. *Fire Sci. Technol.* **2019**, 38, 77–81. [CrossRef]
- 19. Lin, L.; Jian, G.; Xiong, X.-P. Numerical Analysis of Smoke Flow in Tunnel Fire with Single Curvature. *J. Nanchang Hangkong Univ.* (*Nat. Sci. Ed.*) **2019**, *33*, 66–67, 88. [CrossRef]
- 20. Liu, Z.; Chen, C.; Liu, M.; Wang, S.; Liu, Y. Numerical Simulations on the Extinguishing Effect of Water Mist System with Different Parameters of Longitudinal Ventilation in Curve Tunnel Fire. *Adv. Civ. Eng.* **2021**, *5*, 1–13. [CrossRef]
- 21. *JTG/T D70/2-02-2014*; Guidelines for Design of Ventilation of Highway Tunnel. People's Communications Press: Beijing, China, 2014.
- 22. NFPA 502; Standard for Highway Tunnels, Bridges, and Other Limited Access Highways. National Fire Protection Association: Quincy, MA, USA, 2020.
- 23. McGrattan, K.; McDermott, R.; Floyd, J.; Hostikka, S.; Forney, G.; Baum, H. Computational fluid dynamics modelling of fire. *Int. J. Comput. Fluid Dyn.* **2012**, *26*, 349–361. [CrossRef]
- 24. McGrattan, K.; Hostikka, S.; McDermott, R.; Floyd, J.; Weinschenk, C.; Overholt, K. *Fire Dynamics Simulator Users Guide*, 6th ed.; Special Publication (NIST SP)–1019; National Institute of Standards and Technology: Gaithersburg, MD, USA, 2013. [CrossRef]
- 25. Fan, C.; Chen, J.; Zhou, Y.; Liu, X. Effects of fire location on the capacity of smoke exhaust from natural ventilation shafts in urban tunnels. *Fire Mater.* **2018**, 42, 974–984. [CrossRef]
- McGrattan, K.B.; McDermott, R.J.; Weinschenk, C.G.; Forney, G.P. Fire Dynamics Simulator Technical Reference Guide Volume 1: Mathematical Model; NIST Special Publication; National Institute of Standards and Technology: Gaithersburg, MD, USA, 2013. [CrossRef]
- 27. Ji, J.; Gao, Z.H.; Fan, C.G.; Sun, J.H. Large Eddy Simulation of stack effect on natural smoke exhausting effect in urban road tunnel fires. *Int. J. Heat Mass Tran.* **2013**, *66*, 531–542. [CrossRef]
- 28. Zhang, X.-L.; Lin, Y.-J.; Shi, C.; Zhang, J. Numerical simulation on the maximum temperature and smoke back-layering length in a tilted tunnel under natural ventilation. *Tunn. Undergr. Space Technol.* **2021**, *107*, 103661. [CrossRef]

29. Bai, Y.; Zhang, X.-F.; Yan, X.; Zeng, Y. Study on Controlling Velocity under Fire in Two-direction Road Tunnel with High Altitude. *Chin. J. Undergr. Space Eng.* **2019**, *15*, 269–276.

- 30. World Road Association (PIARC). The Highway Tunnels Manual; World Road Association: Pairs, France, 2016.
- 31. Zheng, B.; Fang, L.; Guo, R. Analysis of Longitudinal Temperature Distribution Law and Influencing Factors of High-altitude Tunnel under Unidirectional Ventilation. *Mod. Tunn. Technol.* **2021**, *58*, 349–358. [CrossRef]
- 32. Liu, B.; Mao, J.; Xi, Y.; Hu, J. Effects of altitude on smoke movement velocity and longitudinal temperature distribution in tunnel fires. *Tunn. Undergr. Space Technol.* **2021**, 112, 103850. [CrossRef]
- 33. *JTG D70/2-2014*; Specifications for Design of Highway Tunnels. Section 2 Traffic Engineering and Affiliated Facilities. China Communications Press: Beijing, China, 2014.
- 34. Jafari, S.; Farhanieh, B.; Afshin, H. Numerical investigation of critical velocity in curved tunnels: Parametric study and establishment of new model. *Tunn. Undergr. Space Technol.* **2023**, *135*, 105021. [CrossRef]
- 35. Jafari, S.; Farhanieh, B.; Afshin, H. Effects of Fire Parameters on Critical Velocity in Curved Tunnels: A Numerical Study and Response Surface Analysis. *Fire Technol.* **2024**, *60*, 1769–1802. [CrossRef]
- 36. Pan, R.-L.; Wang, Y.-N.; Yue, S.-Y.; Ran, C.-H.; Cheng, H.-H.; Zhong, M.-H. Full-scale experimental study on longitudinal smoke flow field characteristics in high-speed railway tunnels. *J. Tsinghua Univ. (Sci. Technol.)* **2024**, 1–12. [CrossRef]
- 37. National Railway Administration of People's Republic of China. *Code for Design on Evacuation Engineering for Disaster Prevention and Rescue of Railway Tunnel*; National Railway Administration of People's Republic of China: Beijing, China, 2017.
- 38. Leslie, J.; Millenson, J. Principles of Behavioral Analysis; Prentice Hall: Hoboken, NJ, USA, 1967.
- 39. PIARC Technical Committee Road. Fire and Smoke Control in Road Tunnels; PIARC Technical Committee Road: La Défense, France, 1999.
- 40. National Fire Protection Association. NFPA 72 National Fire Alarm and Signaling Code 2019 Edition; National Fire Protection Association: Boston, MA, USA, 2019.
- 41. Caliendo, C.; Ciambelli, P.; De Guglielmo, M.L.; Meo, M.G.; Russo, P. Simulation of People Evacuation in the Event of a Road Tunnel Fire. Procedia: Social & Behavioral. *Sciences* **2012**, *53*, 178–188. [CrossRef]
- 42. Wang, G.-H.; Yan, Z.-G. Simulation study on evacuation time in long and steep pedestrian cross passage of highway tunnel. *Mod. Tunn. Technol.* **2019**, *s*2, 132–137. [CrossRef]
- 43. *GB 1589-2016*; Limits of Dimensions, Axle Load and Masses for Motor Vehicles, Trailers and Combination Vehicles. General Administration of Quality Supervision, Inspection and Quarantine of the People's Republic of China: Beijing, China, 2016.
- 44. Wang, X.; Qu, J.-R.; Xia, Y.; Wang, L.; Zhen, Y. Study on Evacuation and Rescue of Fire Personnel in Single-Hole Two-Way Highway Tunnel. *J. Undergr. Space Eng.* **2020**, *16*, 944–954.
- 45. Zhang, T.-R.; Li, W.; Yan, Z.-G. Research on Performance of Longitudinal Smoke Extraction Strategy and Personnel Evacuation in Road Tunnel. *Mod. Tunn. Technol.* **2020**, *57*, 651–661. [CrossRef]
- 46. Jones, W.W. State of the art in zone modeling of fires. The Vereinigung zur Forderung desDeutschen Brandschutzes e. V. (VFDB). In Proceedings of the 9th International Fire Protection Seminar, Engineering Methods for Fire Safety, Munich, Germany, 25–26 May 2001; pp. 89–126.

Disclaimer/Publisher's Note: The statements, opinions and data contained in all publications are solely those of the individual author(s) and contributor(s) and not of MDPI and/or the editor(s). MDPI and/or the editor(s) disclaim responsibility for any injury to people or property resulting from any ideas, methods, instructions or products referred to in the content.